

ANALYSIS OF THE FLOW TRAJECTORY AND EMISSION CHARACTERISTICS IN AUTOMOBILE EXHAUST SYSTEM FOR LIGHT-DUTY PASSENGER VEHICLES

I.B. Owunna and A.E Ikpe

Department of Mechanical Engineering, University of Benin, PMB 1154

Abstract

The flow trajectory and emission characteristics in automobile exhaust system for light-duty passenger vehicles was analysed in this study. Delta 1600-V exhaust gas analyser was placed in the tail pipe of the vehicle while regulating the car through European Extra Urban Driving Cycle (EUDC) at a speed range of 1200-3000 rpm and measuring the exhaust gases at each speed range. The experiment was conducted for both diesel and gasoline engine to examine the emission variation. The engine specifications via Finite Element Method (FEM) were employed as input variables to simulate the exhaust flow trajectory and emission characteristics using Solidworks software 2016 version. For the flow trajectory, the exhaust temperature, mass flow rate, velocity and turbulent increased as the engine speed increased. It was noted that the emission characteristics which included HC, CO, CO₂, NO as well as the smoke opacity increased simultaneously with the engine speed. Comparatively, the finding of this study reaffirmed with standard principles of light-duty vehicle in road condition that gasoline engine generates more Green House Gases (GHGs) than diesel engine. With the proximity in both experimentally and FEM determine emission values, this study has indicated that FEM models can effectively predict exhaust emission characteristics provided the engine specifications which serve as the model input variables are accurate.

Keywords: Light-duty vehicle, Exhaust gas, Emissions, Environment, Smoke opacity

1. Introduction

Internal Combustion Engines (ICEs) continue to be relevant in land, air and sea transportation despite the increasing awareness in terms of global pollutant emissions and its effect on the environment. Studies conducted by Karamitros et al. [1], have shown that pollutants emitted from vehicle fleet contributes immensely to the degeneration of air quality, particularly in urban areas where passenger vehicles are basic household necessity. This is due to the combustion process of fuel in IC engines which result in emission of particulate matter, volatile organic compounds, NO_x, CO₂, etc. released from the tail pipe during vehicle operation [2]. Several studies have been carried out in recent times to address these problems, with each study proposing an alternative way of mitigating against the environmental impacts resulting from ICE applications. For example, Pilusa et al. [3] evaluated the effects of using a Whale filter on vehicle exhaust emissions, and found that 35.3% CO, 26.1% NO_x and 34.4% HC reduction can be achieved in exhaust gas emissions. Cho and He [4] investigated the combustion and emission characteristics in a natural gas engine at two different fuel injection timings during the intake stroke. It was observed that late fuel injection timing can reduce the level of CO and HC emissions while the level of NO_x can be reduced only at late fuel injection timing. Oxidation of CO in the reaction process occurs late after all the fuel components and intermediate HC compounds have been burned [5]. The reactions governing NO_x formation is as a result of long resident time, high concentration of oxygen in the mixture as well as high level temperature [6]. Clifford et al. [7] investigated the effectiveness of an optical sensor system for the online measurement of carbon dioxide emissions in the exhaust system of a motor vehicle. The sensor proved to be suitable for monitoring CO₂ concentrations between the range of 2% and 15%, as recorded by commercial gas analyser. Faris et al. [8] analytically developed and validated a model of the steady speed regulated diesel exhaust CO emission rate for trucks. It was found that the steady-speed CO exhaust emission rate is based on CO₂ dissociation, the water-gas shift reaction and the incomplete combustion of hydrocarbon.

Correspondence Author: Owunna I. B., Email: ikechukwu.owunna@uniben.edu, Tel: +2349034983495

Transactions of the Nigerian Association of Mathematical Physics Volume 10, (July and Nov., 2019), 127 –134

Nematizade et al. [9] examined the performance of a gasoline-ethanol blend (E20) and G-series fuel of GSI and GS2 on exhaust emissions of a spark ignition engine (XU7JP/L3). It was found that both HC and CO undergoes 8% and 47% reduction while CO₂ emission increased. The products present in combustion products both inside the cylinder as well as the exhaust depending on the fuel type may include H₂O, NO, OH, H₂, H, N₂, O, CO, CO₂ etc. [10]. However, determining these products require the use of gas analysers or Finite Element Methods which are seldom used due to the variations in the fuel. In this study, FEM was used in modelling and predicting some combusted products from the exhaust manifold, and the results were validated with the products measured experimentally.

1.1. Theoretical Background

Energy balance for the exhaust gas is given by equation (1);

$$\frac{\partial T_g}{\partial t} + u \frac{\partial T_g}{\partial x} = - \frac{\dot{q}_{cv,i}}{\rho_g C_p g V_1} \quad (1)$$

Where, \dot{q} is the heat transfer rate, g is the acceleration due to gravity, cv is convection, cp is the specific heat capacity, ρ is the density, V is the kinematic viscosity.

For the pipe wall, energy balance for single wall exhaust pipe is given by equation (2);

$$\frac{\partial T_p}{\partial t} = \alpha_p \frac{\partial^2 T_p}{\partial x^2} + \frac{\dot{q}_{cv,i} - \dot{q}_{cv,o} - \dot{q}_{rad}}{\rho_p C_p (V_2 - V_1)} \quad (2)$$

$$\frac{\partial T_{p,i}}{\partial t} = \alpha_{p,i} \frac{\partial^2 T_{p,i}}{\partial x^2} + \frac{\dot{q}_{cv,i} - \dot{q}_{cv,gap} - \dot{q}_{rad,i}}{\rho_{p,i} C_{p,i} (V_2 - V_1)} \quad (3)$$

$$\frac{\partial T_{p,o}}{\partial t} = \alpha_{p,o} \frac{\partial^2 T_{p,o}}{\partial x^2} + \frac{\dot{q}_{cv,gap} + \dot{q}_{rad,i} - \dot{q}_{rad,o}}{\rho_{p,o} C_{p,o} (V_4 - V_3)} \quad (4)$$

The convection exhaust gas to pipe wall is given by equation (5);

$$Nu = \frac{\frac{f}{8}(Re-1000)Pr}{1.07+12.7\sqrt{\frac{f}{8}}(Pr^{2/3}-1)} \quad (CAF) \quad (5)$$

Where f is the pipe friction factor, Re is Reynolds number, Pr is Prandtl number, CAF is the Convective Augmentation Factor.

The Convective augmentation factor radiation to surrounds is given by equation (6);

$$\dot{q}_{rad} = \varepsilon \sigma \pi d_2 (T_p^4 - T_{amb}^4) \Delta x \quad (6)$$

Where, ε is the emissivity factor, amb is ambient, x is axial distance from entrance, d is the pipe diameter, σ is Stefan-Boltzmann constant.

The heat transfer coefficient through the exhaust manifold is given by equation (7);

$$h_g = \frac{\dot{Q}}{A_s \Delta T_{lm}} \quad (7)$$

Where, ΔT_{lm} is the logarithmic temperature difference expressed in equation (8);

$$\Delta T_{lm} = \frac{\Delta T_i - \Delta T_o}{\ln\left(\frac{\Delta T_i}{\Delta T_o}\right)} \quad (8)$$

Where, ΔT_i and ΔT_o are the difference in the gas and wall temperature at pipe inlet and outlet.

The molar fractions of compositions in the exhaust gases can be obtained from equations (9-12);

$$\phi_{N_2} = \frac{ak_{N_2}}{1+a+a_0k_{O_2}-\theta_H/2} \quad (9)$$

$$\phi_{O_2} = \frac{(a-a_0)k_{O_2}}{1+a+a_0k_{O_2}-\theta_H/2} \quad (10)$$

$$\phi_{CO_2} = \frac{\theta_C}{1+a+a_0k_{O_2}-\theta_H/2} \quad (11)$$

$$\phi_{H_2O} = \frac{\theta_H/2}{1+a+a_0k_{O_2}-\theta_H/2} \quad (12)$$

Where, k_{N_2} and k_{O_2} are the molar fractions of N₂ and O₂ while θ_C and θ_H are the atomic numbers of carbon and hydrogen in the hydrocarbon fuel.

Considering the aforementioned four compositions (see equation 9-12) as ideal gases, their constant pressure heat capacity can be obtained from the empirical formula [11], in equation (13);

$$C_{p,i} = (C_0 + C_1T + C_2T^2 + C_3T^3 + C_4T^4)R \quad (13)$$

The relationship between a vehicle emission concentration and the specific fuel consumption was established in a study carried out by Heseding and Daskalopoulos [12], as given by equation (14).

$$EP_i = EV_{i,d} * \left(\frac{M_i}{M_{Exh,d}} * \frac{m_{Exh,h}}{P_{eff}} \right) = EV_{i,w} * \left(\frac{M_i}{M_{Exh,w}} * \frac{m_{Exh,w}}{P_{eff}} \right) \quad (14)$$

EP_i is the mass of pollutant, $EV_{i,d}$ is the exhaust emission value of component on dry basis, $EV_{i,w}$ is the exhaust emission value of component on wet basis, M_i is the molecular mass of component, $M_{Exh,d}$ is the molecular mass of exhaust gases on dry basis, $M_{Exh,w}$ is the molecular mass of exhaust gases on wet basis, P_{eff} is the power output.

A variation of the Beer-Lambert Law can be employed in the calculation of exhaust gas concentrations [7] as expressed in equation (15);

$$ppm = \frac{-\left[\ln \frac{I}{I_0}\right] [w \cdot d \cdot 10^6]}{\sigma \cdot N_A \cdot l} \tag{15}$$

Where, σ is the absorption cross section, w is the molecular weight of the gas, d is the density of the gas, N_A is Avogadro's constant, I is the transmitted intensity, I_0 is the incident intensity, l is the optical path length and ppm is the gas concentration in parts per million.

Equation (16) and (17) can be employed to determine the mass production of emissions using values obtained from the Engine Control Unit [13];

$$Q_{mv} = \frac{28,96 \left(P_s - \frac{P_{atm}}{\epsilon} \right) V_z \cdot \eta_d \cdot n}{600 \cdot i \cdot R \cdot T_{vzd}} \tag{16}$$

Where, Q_{mv} is the amount of air aspirated by the engine, 28,96 is the molar mass of air, P_s is the intake pressure, P_{atm} is the atmospheric pressure, ϵ is the engine compression ratio, V_z is the engine capacity, η_d is the engine volumetric efficiency, 600 is the constant conversion unit, i is constant depending on engine type, R is universal gas constant, T_{vzd} is the intake air temperature.

$$M_i = \frac{\left(\frac{Q_{mv}}{28,96} + \frac{Q_{mp}}{14,17} \right) C_i}{100} Q_i \tag{17}$$

Where, M_i is the mass production of emission components, Q_{mp} is the amount of fuel supplied to the engine, C_i is the concentration of one emission component in exhaust gas, 14,17 is the molar mass of fuel, Q_i is the molar weight of one emission component in exhaust gas.

2. Materials and Method

The experimental setup as also demonstrated by Clifford et al. [7] incorporates Delta 1600-V gas analyser which through the help of an optical fibre sensor system detects the exhaust emission contents as it flows through it from the exhaust manifold. As shown in Figure 1, the vehicle was started and the car was regulated following each process of the European Extra Urban Driving Cycle (EUDC) which is used to simulate more aggressive, high speed driving conditions which in this case was in the range of 1200-3000 rpm. Specification of ICEngine used in the experiment is presented in Table 1.

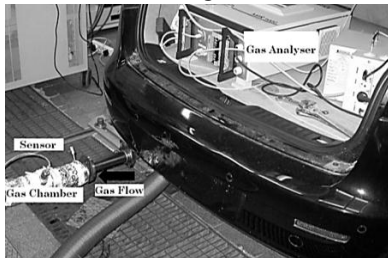


Figure 1: Experimental Setup Showing the Exhaust outlet and Gas Analyser

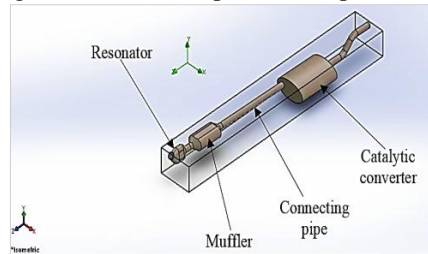


Figure 2: Model of the Exhaust System

Modelling and simulation of the Light-duty passenger vehicle exhaust system was carried out with Solidworks software 2016 version using Finite Element Method (FEM). The exhaust model is shown in Figure 2 while the boundary condition employed in the model simulation is presented in Table 2.

Table 1: Engine Specification (4 Cylinder) for the Experiment

S/N	Parameters	Specification	Engine Speed (n_e) (RPM)	Throttle Position (V_i) (%)
1.	Compression ratio (r)	12.2	1200	21
2.	Expansion coefficient (k)	1.4	1400	21
3.	Max Engine speed (RPM)	3000	1600	25
4.	Bore (mm)	81	1800	25
5.	Mass of piston (lbs)	1	2000	30
6.	Ratio of crank to connecting rod length	0.35	2200	30
7.	Clearance volume (litres)	0.05	2400	36
8.	Mass of connecting rod (lbs)	1.75	2600	36
9.	Max. output (kw rmp ⁻¹)	64/6000	2800	41
10	Stroke (mm)	82	3000	41

Table 2: Boundary Conditions Employed in the Model Simulation

Thermodynamic parameters	Static Pressure: 101325.00 Pa Temperature: 900.00 K
Velocity parameters	Velocity vector Velocity in X direction: 0 m/s Velocity in Y direction: 0 m/s Velocity in Z direction: 0 m/s
Emissions	Carbon monoxide, Carbon dioxide, Nitrogen, Hydrocarbon
Turbulence parameters	Turbulence intensity and length Intensity: 2.00 % Length: 7.620e-004 m
Condition: Inlet Mass Flow	
Type	Inlet Mass Flow
Faces	Face<3>@LID5-1
Coordinate system	Face Coordinate System
Flow parameters	Flow vectors direction: Normal to face Mass flow rate: 0.1000 kg/s Fully developed flow: Yes
Thermodynamic parameters	Approximate pressure: 101325.00 Pa Temperature: 900.00 K
Condition: Environmental Pressure	
Type	Environment Pressure
Faces	Face<4>@LID3-1
Coordinate system	Face Coordinate System
Thermodynamic parameters	Environment pressure: 101325.00 Pa Temperature: 1000.00 K
Turbulence parameters	Turbulence intensity and length Intensity: 2.00 % Length: 7.620e-004 m
Boundary layer parameters	Boundary layer type: Turbulent
Condition: Outer Wall	
Type	Outer Wall
Coordinate system	Global coordinate system
Heat transfer coefficient	300.000 W/m ² /K
External fluid temperature	300.00 K
Fuel	Diesel, Gasoline

3. Results and Discussion

From the finite element simulation carried out in this study, the thermodynamic results of output operating parameters are presented in Table 3 while the thermodynamic results obtained at different engine speeds are tabulated in Table 4.

Table 3: Thermodynamic Results of output Operating parameters

Name	Minimum	Maximum
Pressure [Pa]	101325.00	878145.22
Temperature [K]	511.13	922.28
Velocity [m/s]	0	796.357
Density (Solid) [kg/m ³]	8000.00	8000.00
Mach Number	0	1.62
Relative Humidity [%]	0	1.44
Surface Heat Flux [W/m ²]	-464459.862	158152.809
Heat Flux [W/m ²]	3544.442	1.282e+007
Overheat above Melting Temperature [K]	-3.403e+038	-3.403e+038

Table 4: Thermodynamic Results obtained at Different Engine Speeds

Engine Speed (n_e) (RPM)	Temperature (K)	Mass Flow Rate (m^3/s)	Velocity (m/s)	Turbulent KE (m^2/s^2)* 10^7
1200	300.00	2.254	47.60	3.2
1400	369.14	2.682	88.475	3.6
1600	438.28	3.541	176.950	4.5
1800	507.43	3.874	265.425	4.8
2000	576.57	4.723	353.900	5.7
2200	645.71	5.895	442.376	6.8
2400	714.85	6.714	530.851	7.2
2600	784.00	7.863	619.326	7.7
2800	853.14	8.653	707.801	8.2
3000	922.28	9.754	796.276	9.3

From the colour profile in Figures 3-4, red colour indicates the maximum value, royal blue indicates the minimum value, sky blue represents a value that is higher than that of royal blue, aqua (SVG) blue, green, lemon, yellow and orange represents higher values in ascending order[14]. The flow trajectories showing the velocity of the combusted gases along the exhaust manifold is shown in Figure 3-4. Represented by royal blue colour on the colour profile, the minimum velocity of the exhaust gas at engine speed of 1200 rpm and mass flow rate of 2.254 m^3/s variedly increased from 47.60 m/s to 796.276 m/s at engine speed of 3000 rpm and mass flow rate of 9.754 m^3/s , represented by red colour on the colour profile.

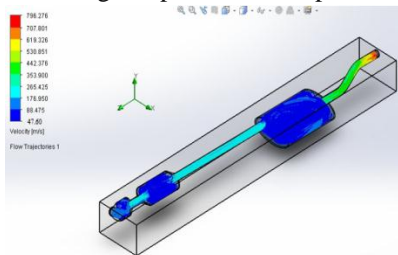


Figure 3: Flow Trajectories showing Velocity of Exhaust Gases along the Manifold

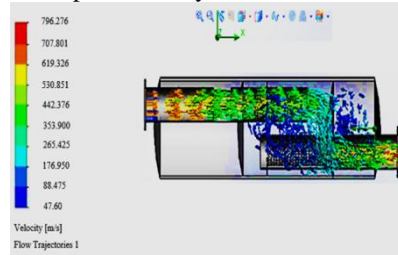


Figure 4: Flow Trajectories showing Velocity of the Exhaust Gases along the Muffler

Figure 5 indicates the flow trajectory of the exhaust gas pressure along the manifold. The colour profile is the same as discussed earlier in the case of velocity. The highest pressure (878145 Pa) designated by red colour is observed at the resonator, followed by the muffler represented by orange colour. Following the colour profile, it can further be observed that the pressure of the combusted exhaust gas along the manifold decreases to minimum value of 101325 Pa at the end of the exhaust pipe before being emitted into the environment. This is because, the exhaust pressure is interrupted by the internal components of the resonator, muffler as well as the somewhat curved geometry of the exhaust pipe, thereby, reducing the exhaust pressure before emission. In scenarios where the engine speed increases constantly or the vehicle continues to fire, this will still be the outcome but the pressure will vary. The flow trajectories showing temperature of exhaust gases along the manifold at road condition is illustrated in Figure 6.

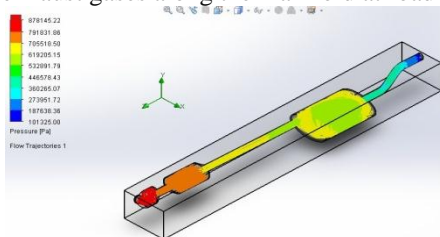


Figure 5: Flow Trajectories showing Pressure of Exhaust Gases along the Manifold

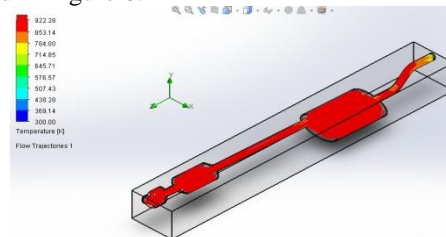


Figure 6: Temperature Flow Trajectories of Exhaust Gases along the Manifold

As mentioned earlier, red colour in Figure 7-8 indicates the highest temperature distribution on the exhaust material, royal blue indicates the minimum temperature on the exhaust material, sky blue indicates the temperature at which the exhaust material begins to respond to the exhaust temperature, aqua (SVG) blue, sky blue, yellow, lemon and orange colour

indicates further responses of the exhaust material to the exhaust temperature. Figure 7 represents the temperature trajectories of the combusted gases exiting the combustion chamber at full load in road condition. In real life scenario, the exhaust temperature at idle mode and in the beginning of a journey will vary from ambient temperature (33-45°C) through moderate temperature (50-250°C) to high and extremely high temperature (300-900°C) when the exhaust temperature increases gradually as the driving distance, time as well as the engine speed increases. The relationship between the colour profile and temperature level is that at engine idle mode (ambient temperature), the colour is royal blue and at road condition where the vehicle operates at full engine load, the colour changes to red which signifies peak temperature and peak engine load. Figure 8 represents flow trajectory of the exhaust gases along the exhaust muffler. The red colour represents temperature of the hot exhaust gases coming out of the combustion chamber and entering the muffler inlet, but as it travels along the main chamber begins to reduce gradually until it exits the muffler outlet which is represented by royal blue and sky blue.

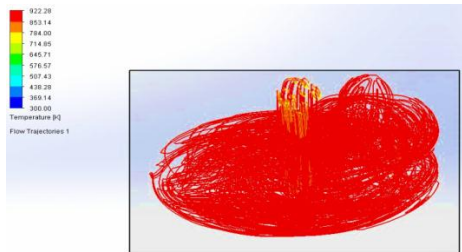


Figure 7: Temperature Flow Trajectory of Hot Combusted Gases Exiting Combustion Chamber

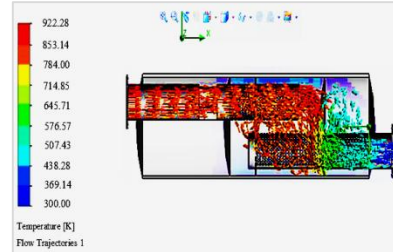


Figure 8: Temperature Flow Trajectory of Exhaust Gases along the Muffler

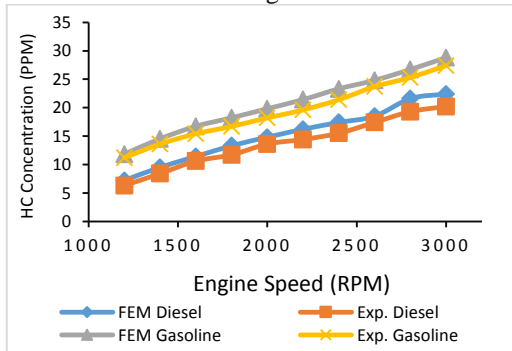


Figure 9: Plot of HC Concentration against Engine Speed

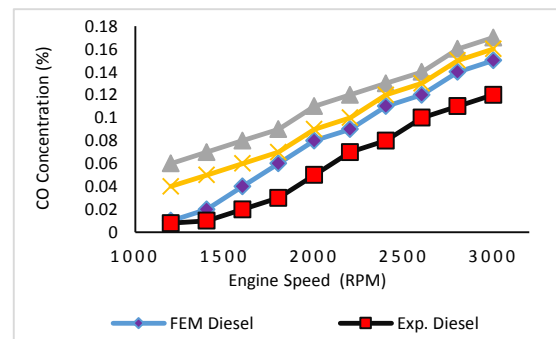


Figure 10: Plot of CO Concentration against Engine Speed

Figure 9 represents a plot of HC concentration against engine speed which indicates that HC emission increases simultaneously with engine speed. Hydrocarbons (HCs) are emitted from vehicle exhausts as unburnt fuel and also through the process of evaporation from the fuel tank. High emissions of HC during driving test or high idle test can occur as a result of vacuum leaks, malfunction of ignition system, faulty air injection system, internal engine problem, failed catalytic converter etc. On the other hand, high HC at idle mode can occur due to ignition system malfunction, incorrect air/fuel mixture, vacuum leaks, incorrect ignition timing and/or idle speed, EGR valve partially stuck open, faulty fuel injection system, inoperative catalytic converter, air injection system failure etc.

Figure 10 represents a plot of CO concentration against engine speed which indicates that CO emission is directly proportional to engine speed. Carbon monoxide is one of the major toxic compounds emitted from auto exhaust systems due to improper combustion of air-fuel mixture in their operation cycle. High emissions of Carbon monoxide (CO) on driving test or high idle test (excessively rich mixture) can occur due to carburettor malfunction, dirty air filter or faulty choke, faulty fuel injection system, faulty thermostatic air cleaner system, defective evaporative canister purge system, inappropriate catalytic converter, faulty air injection system etc. On the other hand, high CO at idle mode (excessively rich mixture) can occur due to maladjusted idle mixture, dirty air fuel filter or faulty choke, faulty fuel injection system, excessive fuel pump pressure, faulty air injection system, defective evaporative canister purge system etc.

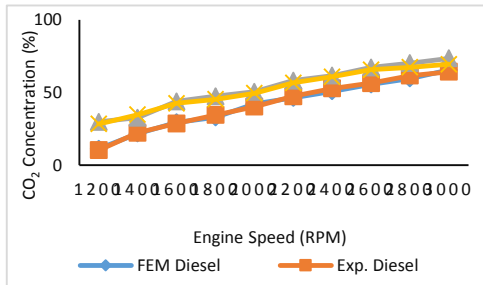


Figure 11: Plot of CO₂ Concentration against Engine Speed

Figure 11 represents a plot of CO₂ concentration against engine speed which indicates that CO₂ emission increases simultaneously with engine speed. Some of the primary constituents of gasoline are carbon and hydrogen atoms. During combustion of air-fuel in the cylinder, Carbon (C) content in the fuel reacts with oxygen in air to produce Carbon dioxide (CO₂) [15]. CO₂ due to its emission from auto exhaust systems is a major Green House Gas that contributes to climate change, global warming, cardiovascular diseases in human, acidification of oceans etc. As a result of that, European Commission has laid down targets designed to limit the extent of CO₂ emission into the atmosphere. However, the amount of CO₂ emitted by automobile systems is directly connected to the amount of fuel it consumes, therefore, vehicles with lower CO₂ emission are more efficient in fuel consumption.

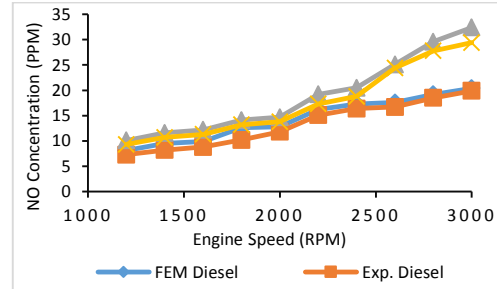


Figure 12: Plot of NO Concentration against Engine Speed

Figure 12 represents a plot of NO concentration against engine speed which indicates that NO emission increases simultaneously with engine speed. When the Nitrogen and oxygen from auto emissions mix together, a toxic compound is formed known as Nitrogen oxide which can react with HCs to produce low level ozone which can cause inflammation of the airways. As this compound is released into the atmosphere, the condition may contribute to acid rain. High emissions of Nitrogen oxide (NO) on driving test can occur due to inoperative/ineffective Exhaust Gas Recirculation (EGR) system, excessively lean/fuel ratio, faulty catalytic converter, excessive spark advance, faulty thermostatic air cleaner system, faulty cooling system etc.

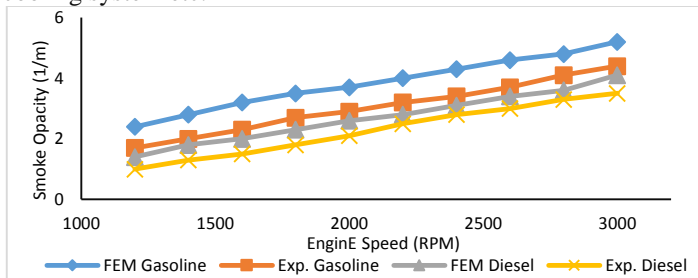


Figure 13: Plot of Smoke Opacity against Engine Speed

Figure 13 indicates that smoke opacity increases as the engine speed increase. This is evidence in both experimentally determined and FEM modelled smoke opacity with corresponding engine speeds for diesel and gasoline engine. This is because as the engine speed increases, the more momentum is required to propel the car, as such the rate at which fuel is supplied to the carburettor increase likewise the noise level as well as the overall temperature of car.

4. Conclusion

Comparing the FEM and experimentally determined exhaust emissions in this study, a close similarity was observed in the emission values. Moreover, graphical representation of the FEM and experimental emission results exhibited similar trend. This indicates that if the right engine specifications are employed effectively in modelling and prediction of vehicle exhaust emission characteristics, the output results may likely be very close to actual case scenario. This can save time, energy and resources required to accurately achieve the same set of results using experimental approach.

References

- [1] Karamitros, D., Skarlis, S. A. and Koltsakis, G. (2014) Exhaust Gas After-treatment Technologies and Model Based Optimization. Chapter 5, Automotive Exhaust Emissions and Energy Recovery, Nova Science Publishers Inc, ISSN: 978-1-63321-493-4.
- [2] Sarkan, B., Stopka, O., Gnap, J. and Caban, J. (2017) Investigation of Exhaust Emissions of Vehicles with the Spark Ignition Engine within Emission Control. *Procedia Engineering*, 187, 775-782.

- [3] Pilusa, T. J., Mollagee, M. M. and Muzenda, E. (2012) Reduction of Vehicle Exhaust Emissions from Diesel Engines using the Whale Concept Filter. *Aerosol and Air Quality Research*, 12, 994-1006.
- [4] Cho, H. M. and He, B. (2009) Combustion and Emission Characteristics of a Natural Gas Engine Under Different Operating Conditions. *Environmental Engineering Research*, 14(2), 95-101.
- [5] Larsen, J. F. and Wallace, J. S. (1997) Comparison of Emissions Efficiency of a Turbocharged Lean-burn Natural Gas and hythane-fuel Engine, *Transactions of the ASME*, 119(1), 218-226.
- [6] Heywood, J. B. (1998) *International Combustion Engine Fundamentals*, McGraw-Hills, New York.
- [7] Clifford, J., Mulrooney, J., Dooly, G., Fitzpatrick, C., Lewis, E., Merlone-Borla, E. and Flavia, G. (2008) On Board Measurement of Carbon Dioxide Exhaust Car Emissions Using a Mid-Infrared Optical Based Fibre. *IEEE Sensors Conference*, 914-918.
- [8] Faris, W. F., Rakha, H. A. and Elmoselhy, S. (2016) Validated Analytical Modelling of Diesel Engine Regulated Exhaust CO Emission Rate. *Advances in Mechanical Engineering*, 8(6), 1-15.
- [9] Nematizade, P., Ghobadian, B., Ommi, F. and Najafi, G. (2013) Performance and Exhaust Emissions of a Spark Ignition Engines Using G-series and E20 Fuels. *International Journal of Automotive Engineering and Technologies*, 2(2), 55-63.
- [10] Yamin, J.A., Gupta, H. N. and Bansal, B. B. (2003) The Effects of Combustion Duration on the Performance and Emission Characteristics of Propane-fueled 4-Stroke S. I. Engines. *Emirates Journal for Engineering Research*, 8(1), 1-14.
- [11] Shen, W. D., Jiang, Z. M. and Tong, J. G. (2001) *Engineering Thermodynamics*, Third Edition, Higher Education Press, Beijing.
- [12] Heseding, M. and Daskalopoulos, P. (2006) *Exhaust Emission Legislation-Diesel and Gas Engines*. VDMA, Frankfurt am Main.
- [13] Matusu, R., Mik, J. and Kotek, M. (2014) Mathematical Model of the Emissions of a Selected Vehicle. *Journal of Middle European Construction and Design of Cars*, 1, 16-24.
- [14] Owunna, I. B., Ikpe, A. E. and Achebo, J. I. (2019) Temperature and Time Dependent Analysis of Tungsten Inert Gas Welding of Low Carbon Steel Plate using Goldak Model Heat Source. *Journal of Applied Science and Environmental Management*, 22(11), 1719-1725.
- [15] Drabik, D., Mamala, J., Smieja, M. and Praznowski, K. (2017) Possibility of Reducing CO₂ Emissions from Internal Combustion Engines. *E3S Web of Conferences*, 19, 01013.